Journal of Hydrology 438–439 (2012) 97–111

Contents lists available at SciVerse ScienceDirect

Journal of Hydrology

journal homepage: www.elsevier.com/locate/jhydrol

Geochemical and isotopic (oxygen, hydrogen, carbon, strontium) constraints for the origin, salinity, and residence time of groundwater from a carbonate aquifer in the Western Anti-Atlas Mountains, Morocco

N. Ettayfi [a], L. Bouchaou [a,*], J.L. Michelot [b], T. Tagma [a], N. Warner [c], S. Boutaleb [a], M. Massault [b], Z. Lgourna [a], A. Vengosh [c]

[a] Applied Geology and Geo-Environment Laboratory, Ibn Zohr University, Agadir, Morocco
[b] UMR «IDES», CNRS – Université Paris-Sud, Orsay, France
[c] Division of Earth & Ocean Sciences, Duke University, Durham, NC, USA

ARTICLE INFO

Article history:
Received 5 December 2011
Received in revised form 29 February 2012
Accepted 4 March 2012
Available online 17 March 2012
This manuscript was handled by Laurent Charlet, Editor-in-Chief, with the assistance of P.J. Depetris, Associate Editor

Keywords:
Isotopes
Geochemistry
Groundwater
Salinity
Residence time
Semi-arid

SUMMARY

Groundwater in many arid basins, particularly in developing countries, is the only available water resource that sustains local communities. Yet, information on the basic hydrological parameters and the sustainability of the groundwater exploitation are often lacking. This study investigates the origin of groundwater from the Lower Cambrian carbonate aquifer of the Lakhssas Plateau in the Anti-Atlas Mountains of southwestern Morocco. The study aims to reveal the origin of the groundwater, salinity sources, and the residence time of the water. The study is based on a comprehensive geochemical and isotopic (oxygen, hydrogen, carbon, and strontium) investigation of groundwater from different parts of the basin. The hydrochemical and isotopes results indicated three types of groundwater in the Lakhssas Plateau: (1) thermal water in the southern part of the basin with solute composition that reflects dissolution of calcium–sulfate and calcium carbonate minerals; (2) low-temperature groundwater at the southern margin of the basin with low salinity (chloride content up to 100 mg/L) and chemical composition that is expected from equilibrium with limestone–dolomite rocks; and (3) low-temperature groundwater in the northern, western, and eastern margins of the basin with a wide range of salinity (chloride up to 800 mg/L). The different water types had also different stable isotope composition; the thermal water was depleted in ^{18}O and ^{2}H ($\delta^{18}O$ as low as −7.6‰) relative to the southern (−5.9 to −5.3‰) and northern waters (−5.7 to −3.8‰). The differences in $\delta^{18}O$ and $\delta^{2}H$ between the southern and northern waters are related to elevation that induced fractionation of oxygen and hydrogen isotopes in recharge water originated from coastal moisture. The data suggest that the high salinity in groundwater from the northern, western and eastern margins of the Lakhssas Plateau is related to the presence of schist rocks in these areas. The distinctive low Na/Cl and Br/Cl ratios, coupled with high silica contents and high $^{87}Sr/^{86}Sr$ ratios (up to 0.713) in the saline groundwater provide additional evidences for the link between salinity and the schist rocks. In contrast, the thermal water had relatively low $^{87}Sr/^{86}Sr$ ratio (0.7089), which is identical to the secular seawater Sr isotope ratio during the Early Cambrian period and presumably reflects interaction with the Early Cambrian carbonate and sulfate aquifer rocks. In the northern and southern groundwater, the $^{87}Sr/^{86}Sr$ ratios were higher and correlated with the Mg/Ca ratios, inferring mixing between the Early Cambrian limestone and other rocks with higher $^{87}Sr/^{86}Sr$, such as the schist rocks. The radiocarbon data showed ^{14}C activities ranging from 6 pmC in the thermal water to 62 pmC in the southern water. Age-modeling, corrected for dissolution of the carbonate rocks with dead carbon, simulated mean residence time of 10–15 ka BP for the thermal water and a range of 0 to 3 ka BP for the northern and southern waters, depending on the used models. The integration of the data enables us to establish a conceptual model for the origin of groundwater in the Lakhssas Plateau: (1) recharge to the aquifer from relatively heavy-isotope depleted recharge water, presumably during wetter conditions about 10–15 ka BP. The recharge water interacted at high depth with limestone and calcium sulfate minerals and emerged to the surface as thermal water at the southern part of the basin; (2) more recent recharge from coastal moisture originated from the Atlantic Ocean. The stable-isotope composition of groundwater was controlled by the elevation of their recharge areas: recharge at higher

* Corresponding author. Tel.: +212 6 66 76 91 95; fax: +212 5 28 22 01 00.
E-mail addresses: ettayfi.najat@gmail.com (N. Ettayfi), lbouchaou@gmail.com (L. Bouchaou), jean-luc.michelot@u-psud.fr (J.L. Michelot), tariktagma@yahoo.fr (T. Tagma), nathaniel.warner@duke.edu (N. Warner), saidboutaleb1@yahoo.fr (S. Boutaleb), marc.massault@u-psud.fr (M. Massault), lg.zineb@yahoo.fr (Z. Lgourna), vengosh@duke.edu (A. Vengosh).

http://dx.doi.org/10.1016/j.jhydrol.2012.03.003

elevation, particularly in the southern margin resulted in lower $\delta^{18}O$ and δ^2H values; (3) the recharge water interacted with the carbonate aquifer rocks, particularly with calcite and dolomite minerals. In areas of exposure of schist rocks, the water–rock interaction induced salinization of the groundwater. Overall, our data reveal that the limited water resources in this semi-arid zone of Morocco could be in some parts less renewable and also saline. Future exploitation of this basin will have to account the salinity factor and the suggested contribution of water recharged some thousands years ago.

1. Introduction

The study of water resources in arid areas is becoming increasingly important because of increasing demands and depletion of water resources in these areas. In many parts of the developing world there is no systematic monitoring of the hydrological systems and thus water level decline and degradation of water quality are typically noticed only at evolved stages of aquifer deterioration. This present study investigates the geochemistry of groundwater from the arid to semi-arid area of Lakhssas Plateau in the Anti-Atlas Mountains of southwestern Morocco, where groundwater resources are vital for the local populations, supplying drinking water, irrigation, and sustaining the oasis ecosystems in southern–western Morocco. The Lakhssas Plateau (Fig. 1) consists of Paleozoic limestone that forms a regional carbonate (karst) aquifer which discharge through several springs. The economic growth of the region is directly linked to the development of oasis agriculture and tourism, which both weigh heavily on water reserves in the region. The lack of information regarding the recharge of the aquifer could affect its quantity and quality upon inadequate utilization and poor management.

The Lakhsas area has been the subject of several geological and structural studies (e.g. Belfoul, 2005; Oliva, 1977; Soulaimani, 1998; Soulaimani et al., 2005), which highlighted some structural models in this area of Anti-Atlas Mountains (Fig. 1). Corresponding hydrogeological studies were limited, however, and only included reports carried out by the Hydraulic Agency of Souss-Massa-Draa basin (Agence du Bassin Hydraulique du Souss-Massa-Draa, 2004, 2006). These reports focused mainly on the inventory of the springs and wells in the area with few measurements of springs' flow rates (Agence du Bassin Hydraulique du Souss-Massa-Draa, 2004, 2006). Exploitation of groundwater for drinking water supply in this aquifer began in the 1980s, but the pumping tests at the majority wells have shown very low yield (Agoussine, 1991). Consequently, hydrogeological studies based on only hydrological monitoring of springs are not sufficient to characterize the aquifer system and project its sustainability. Using hydrogeochemical and isotopic methods could bridge this knowledge gap and provide insights on the recharge sources, residence time and sustainability of water exploitation (Azzaz et al., 2007; Barbieri et al., 2005; Bouchaou et al., 2008, 2009; Han and Liu, 2004; Marfia et al., 2004).

This paper provides a comprehensive analysis of water resources in Lakhssas Plateau in the Anti Atlas of Morocco through an evaluation of multiple geochemical (major elements) and isotopic tools ($\delta^{18}O$, δ^2H, $^{87}Sr/^{86}Sr$, $\delta^{13}C$, and $A^{14}C$) in order to evaluate the origin, salinity, and the residence time of the groundwater. In

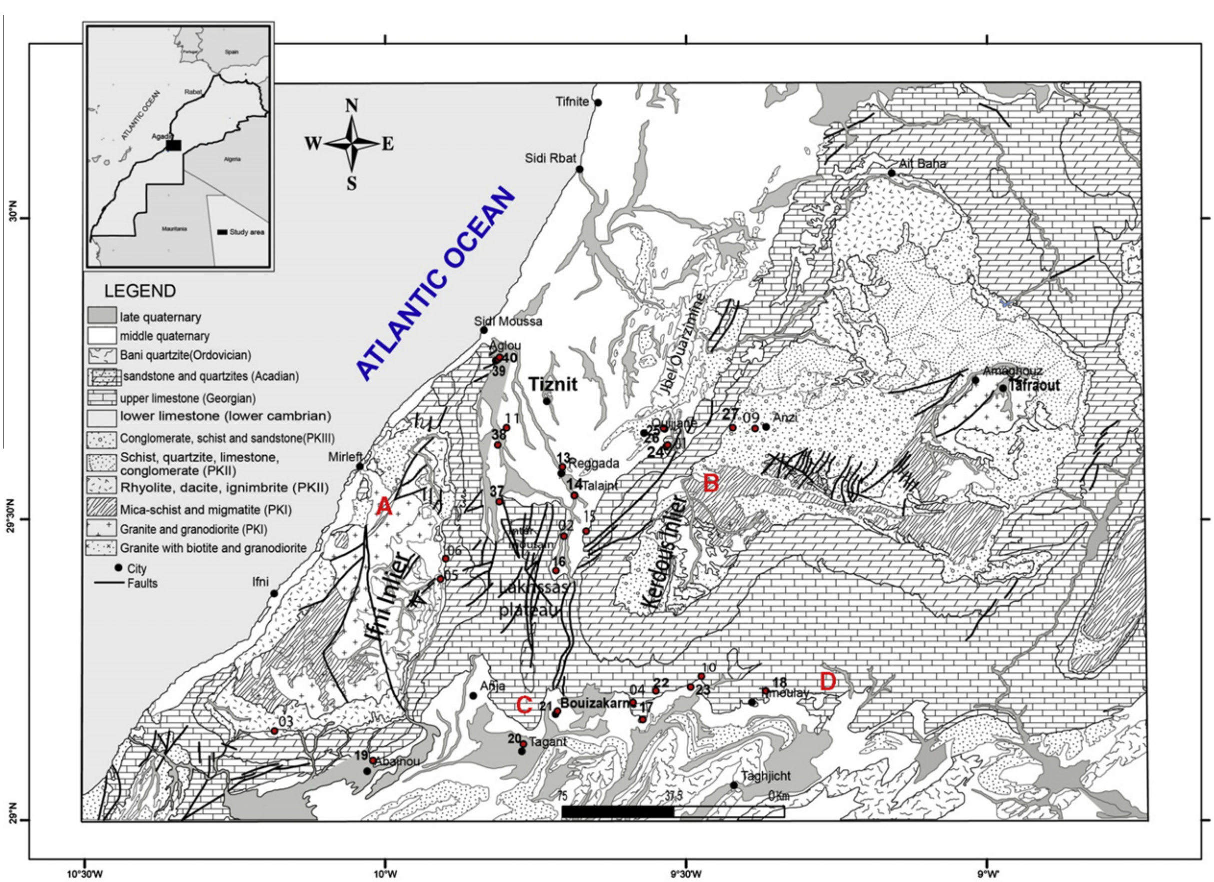

Fig. 1. Location map and geological sketch map of the Lakhssas Plateau area (from geological map 1/500,000 of Marrakesh).

particular, this study is focused on an evaluation of the role of water–rock interactions on the water quality and the apparent residence time detected by radiocarbon dating. These evaluations are crucial for sustainable exploitation in a semi-arid region with very limited water resources.

2. Geological and hydrogeological setting

Lakhssas Plateau is a Cambrian carbonate entablature, outcropping in the South-Western part of the Anti-Atlas as a high plateau between Kerdous and Ifni Inliers. It separates Tiznit plain to the North from Bouizakarne plain to the South (Fig. 1) and extends over 47 km meridian length by about 30 km width and rises up to about 1000 m.a.s.l.

Lakhssas Plateau is part of a semi-arid area with an average annual rainfall of about 150 mm/yrs. Temperature average is about 15 °C in the winter and 35 °C in the summer.

The stratigraphy of the Lakhssas area is composed of late Proterozoic-Cambrian carbonate rocks overlying a crystalline basement (Kerdous in the east, Ifni in the west) through a major unconformity. The basement is composed of granites and metamorphic paleoproterozoic gneisses (Kerdous group) overlain by neoproterozoic quartzite and carbonate series (Lkest group) (British geological Survey, 2001; Barbey et al., 2004; Charlot, 1978). The metamorphic substratum is covered by volcano-sedimentary series of PII_3 group, followed by those of PIII group that belong to upper Neoproterozoic (Hassenforder, 1987).

In this area, the transition from paleoproterozoic volcano-clastic formation to Lower Cambrian series is underlined by weak erosional unconformity (Pique et al., 1999; Soulaimani et al., 2003). The Cambrian series, from the bottom upwards consists of, green siltites and pelitic sandstones (basic series) then dolomites and marls (lower limestone series) and finally dolomitic limestone with red sandy dolomites ("lie de vin" series), which forms the medial part of anticlines toward the center of plateau. Finally rest the superior limestone series, and then the schisto-limestone series. The paleozoic series also depose the middle Cambrian schists formations that occupies synclines centers and westerner feijas (syncline of Tiznit and Bouizakarne) (Fig. 2).

Lakhssas Plateau displays tectonic movements that belong to Hercynian orogenesis. During this event, the area was structured according to a wide synclinorium (Fig. 3). This synclinorium shows globally strong deformation in the center of the plateau basically along subvertical faults; particularly those that line the Jbel inter anticline borders (Fig. 1).

Sedimentary series of Lakhssas Plateau are crossed by an important fault network, which continues under both plains of Tiznit and Bouizakarne. The main structural lines are N–S trending, from low Draa basin in the South, toward Souss basin in the North (Soulaimani and Bouabdelli, 2005; Soulaimani and Burkhard, 2008). It is worth mentioning the great fault affecting the western fallout of Kerdous anticline, which connects at southeast of Ouijjane the Lower Cambrian limestone and Acadian schist.

Historically, the flow rate (1983–2002) recorded by some springs on the northern edge of the plateau does not show significant variations through the years (Fig. 4), apart during exceptional rainfall when increased flow rate was recorded. It seems that these flow rates are supported by deep circulation of a probable old groundwater, channeled into the faulted system of the paleoproterozoic basement described above.

3. Materials and methods

The major springs and several wells of the Lakhssas Plateau were sampled in October 2008, January 2009 and May 2010. Samples were collected in the northern area ($n = 23$), southern area ($n = 16$), western area associated with granitic/metamorphic area of Ifni Inlier ($n = 6$), and eastern area associated with older granitic areas of Kerdous inlier ($n = 5$) (Fig. 1). Fifty samples were analyzed for full major elements composition, subsets of 32, 11, and 14 samples were measured for isotopes of oxygen and hydrogen, carbon (^{14}C and $\delta^{13}C$), and strontium, respectfully. Electrical conductivity (EC), pH, Temperature and bicarbonate are measured in the field. Samples were refrigerated before transport to the various laboratories.

Chemical analysis samples of 2009 were conducted in laboratories in Duke University, USA. Ca, Mg, Na, Sr, Ba, Fe, Mn, and Si concentrations were determined by direct current plasma optical emission spectrometry (DCP) and K was determined by flame atomic absorption spectrometry. Major anion (Cl, NO_3, and SO_4) concentrations were determined by ion chromatography (IC), and bicarbonate concentrations were determined by titration to pH 4.5.

Chemical analysis of 2008 and 2010 samples was conducted at the Applied Geology and Geo-Environment Laboratory, Ibn Zohr University, Agadir Morocco, using methods of volumetric dosage for HCO_3, Ca, Mg and Cl, flame photometer for Na and K and spectrophotometer for SO_4 and NO_3.

Stable isotopes of oxygen and hydrogen were analyzed at the IDES Laboratory of Paris-Sud University, Orsay, France. The results for stable isotopes are expressed in the conventional δ notation in ‰ versus V-SMOW with a reproducibility of ±0.1‰ for $\delta^{18}O$ and ±1‰ for δ^2H.

Stable isotopes of carbon ($\delta^{13}C$ ‰ versus V-PDB) were also measured at the IDES Laboratory, with a precision of 0.15‰. The ^{14}C concentrations were determined by accelerator mass spectrometry (Artemis facility, UMS LMC14, Saclay, France, in the framework of INSU national service) on Fe-graphite targets prepared at the IDES Laboratory. The results are reported in percent modern carbon (pmC), with the uncertainty for each sample.

Strontium isotopes were analyzed by thermal ionization mass spectrometer (TIMS) at Duke University. Water samples were evaporated in a HEPA filtered clean hood. Samples were then digested in 0.55 mL of 3.5 N HNO_3 and then passed through an Eichrom Sr-specific ion exchange resin to separate Sr prior to the isotopic measurement. The separated Sr isotopes were dried with H_3PO_4 and loaded onto out-gassed single rhenium filaments along with 2uL TaO activator solution. All acids used in the separation process were of Optima grade, water was quartz distilled (QD). Samples and standards (NIST987) were then gradually heated to obtain a ^{88}Sr beam intensity of $\sim$3 V, after which 300 cycles of isotope ratio data were collected, yielding a typical internal precision of $\sim$0.000004 for $^{87}Sr/^{86}Sr$ ratios (1 sd). The external reproducibility on the NIST987 standard yielded a mean $^{87}Sr/^{86}Sr$ ratio of 0.710233 ± 0.000009 (1 sd).

4. Results

Tables 1 and 2 show chemical and isotopic data from the different sampling campaigns. The data and following discussion are presented according to geographical and geological distribution of sampling sites in the plateau (Fig. 1). We defined five water groups: (1) northern group – samples that were collected from wells and springs at the northern part of the Lakhssas Plateau within the carbonate aquifer; (2) southern group – samples that were collected from wells and springs at the southern area of the Lakhssas Plateau within the carbonate aquifer; (3) geothermal water (temperature > 30 °C); (4) samples located at the western margin of the Lakhssas Plateau associated with the granitic rocks of Ifni Inlier; and (5) samples located at the eastern margin of the Lakhssas Plateau associated with the granitic rocks of Kerdous Inlier (Fig. 1).

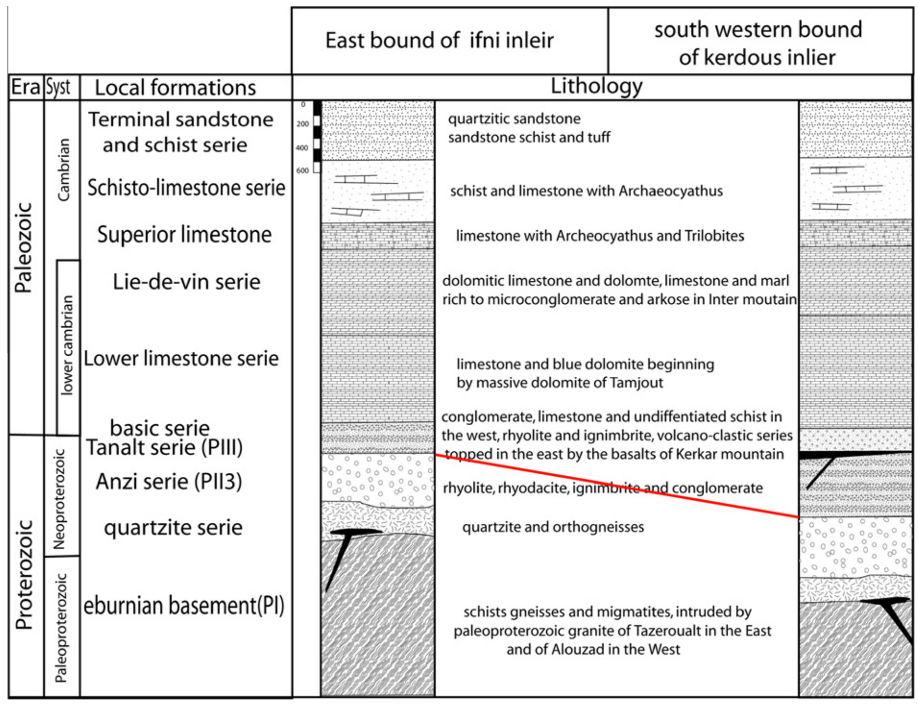

Fig. 2. Lithostratigraphic column of the Lakhssas Plateau area (Soulaimani, 2005).

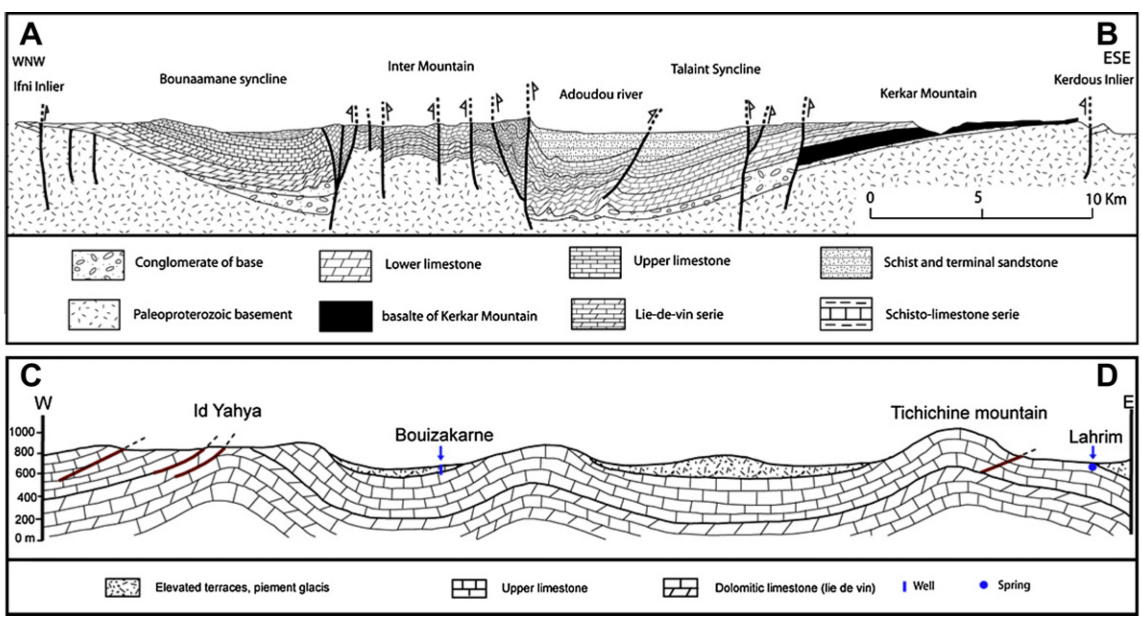

Fig. 3. Synthetic geological cross-section of the northern and southern parts of the Lakhssas Plateau (see location of A, B, C and D in Fig. 1).

4.1. Physical and chemical characterization

The overall salinity (expressed by TDS) and temperature variations (Fig. 5) showed that the thermal water located at the southern part of the Lakhssas Plateau had the highest salinity, about three times relative to the low-temperature water samples. Wells and springs from the western (Ifni Inlier) and eastern (Kerdous Inlier) margins of the basin had the next highest salinity (Fig. 5), followed by samples collected from the north and finally the southern samples had the lowest salinity in general. All water samples from the Lakhssas Plateau were generally characterized by a neutral pH.

To better illustrate the different chemical composition of the five water types, we plotted the chemical data in a Piper diagram (Fig. 6); the groundwaters of the Lakhssas Plateau showed strong variations in the space: Ca–Mg–HCO_3 water type dominated in the south and north edges of the plateau, whereas Ca–SO_4 composition characterized the thermal springs and mixed water type with chloride as the major anion were observed in the western (Ifni Inlier) and eastern (Kerdous Inlier) margins of the basin.

Variations of the major elements as compared to chloride showed that the northern water type had distinctively high chloride (as high as 800 mg/L), sodium, calcium, magnesium, and nitrate contents relative to those of the southern water type. The

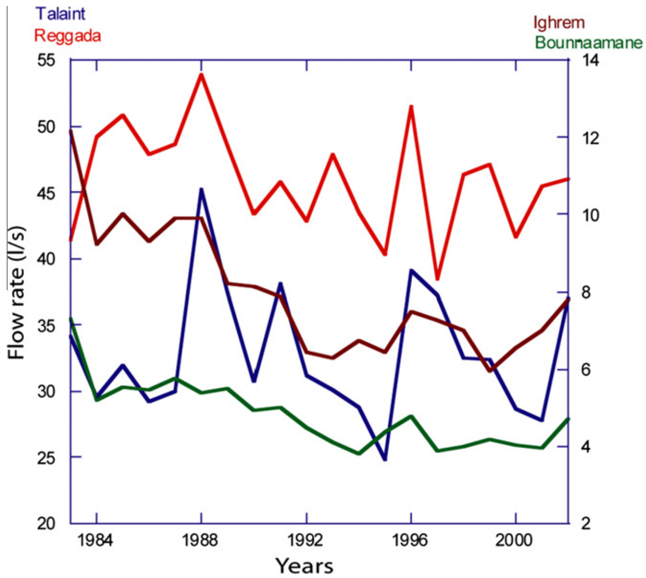

Fig. 4. Variations with time (1983–2002) of the flow rate of four springs situated in the northern part of the Lakhssas Plateau.

thermal water was characterized by predominance of calcium and sulfate (molar Ca/SO_4 ratio of 0.8–0.9; Ca and SO_4 represented 77% of the total dissolved constituents) with relatively high contents of potassium, sodium, and magnesium. Water samples from the western and eastern margins of the basin had high chloride (820 mg/L), sodium (molar Na/Cl ratio of 0.6–0.8), and magnesium contents similar to those of water samples from the northern group (Fig. 7 and 8).

In contrast, bicarbonate contents were higher in the low-saline groundwater of the northern and southern sections and the bicarbonate content decreased with increasing chloride content (Fig. 7). Overall, the sum of bicarbonate, calcium and magnesium in the southern group consisted up to 70% of the total dissolved constituents.

4.2. Isotopic characterization

The isotopic composition of the Lakhssas groundwater ranged from −53.4 to −21.0‰ V-SMOW for δ^2H and from −7.62 to −3.83‰ V-SMOW for $\delta^{18}O$. The δ^2H–$\delta^{18}O$ relationship for all water samples was defined in relation with Global Meteoric Water Line (GMWL), given by the following equation: $\delta^2H = 8\ \delta^{18}O + 10$ (Craig, 1961) (Fig. 9). From a study conducted by Bouchaou et al. (in press), which included measurements of stable isotopes in precipitation from the Souss-Upstream station (1000 m.a.s.l.), we defined the local meteoric water line ($\delta^2H = 8\ \delta^{18}O + 14$) that is representative of the studied area. This line is very close to that defined by Raibi et al. (2006, in Ait Lemkademe et al., 2011) for precipitation over the High-Atlas Mountains ($\delta^2H = 8\ \delta^{18}O + 13.5$), and is also similar to the "Moroccan" meteoric water line established by Ouda et al. (2004) in central Morocco ($\delta^2H = 8\ \delta^{18}O + 13$). Fig. 9 shows that the samples of Lakhssas groundwater plot close to this local meteoric water line. Deuterium excess values (d-excess), calculated as $d = \delta^2H - 8\ \delta^{18}O$ ranged from 7‰ to 14‰, with most values higher than 10‰. As the air masses originate mainly from the Atlantic Ocean, the relatively high deuterium excess values suggest significant contributions of recycled continental water vapor to rainfall (Clark and Fritz, 1997).

Water from the northern region had distinctively higher $\delta^{18}O$ and δ^2H values relative to the southern type and thermal waters. The geothermal water had lower $\delta^{18}O$ and δ^2H values ($\delta^{18}O$ as low as −7.6‰). The relationship between chloride and $\delta^{18}O$ (Fig. 10) showed that the northern water had both high salinity and higher $\delta^{18}O$. Water samples with chloride content below 200 mg/L showed a linear correlation between Cl and $\delta^{18}O$ values.

The $^{87}Sr/^{86}Sr$ ratios of northern and southern water types were similar (range of 0.7093–0.7105) with one exception of higher $^{87}Sr/^{86}Sr$ ratio (sample from the north with 0.7130). A trend of decreasing $^{87}Sr/^{86}Sr$ ratios with Sr content was observed for the southern water types (Fig. 11). The thermal water had lower $^{87}Sr/^{86}Sr$ ratios of 0.70890–0.70897. The HCO_3^- contents, $\delta^{13}C$ values, and $A^{14}C$ activities of the northern waters were different from the southern part; the northern water had higher bicarbonate content, higher $\delta^{13}C$ values (−9.8‰ to −7.5‰) and lower $A^{14}C$ activities (40–50 pmC) relative to the southern water with lower bicarbonate content and $\delta^{13}C$ values (−10.3‰ to −10.8‰) and higher $A^{14}C$ activities (54–63 pmC). The thermal water had significantly higher $\delta^{13}C$ values (−5.7‰) and lower $A^{14}C$ activities (6 pmC). Variations of $\delta^{13}C$ versus $A^{14}C$ showed inverse correlation for the northern water (Fig. 12).

4.3. Geochemical modeling

Since the major aquifer lithology of the Lakhssas Plateau is composed of carbonate rocks, we calculated the saturation level of the water samples with respect to different carbonate minerals. Generation of carbon dioxide, in the soil upon recharge could react with the carbonate rocks in the aquifer, dissolving calcite and dolomite according to the following reactions:

$$2CaCO_3 + 2CO_2 + 2H_2O = 2Ca^{2+} + 4HCO_3^-$$

$$CaMg(CO_3)_2 + 2CO_2 + 2H_2O = Ca^{2+} + Mg^{2+} + 4HCO_3^-$$

Saturation indexes were calculated by *Diagrammes ® version 5*; a computer program for hydrochemical calculations (Smiler, 2005). The results of the calculations showed that almost all the water samples were over-saturated with respect to both dolomite and calcite (Fig. 13). Saturation indexes for all plateau waters ranged from 0.05 to 1.12 for calcite and from 0.01 to 2 for dolomite (Table. 1). An additional indication for the dolomite contribution was the relationship of Mg/Ca molar ratio (between 0.27 and 1.08) and HCO_3 in a binary diagram (Fig. 13). The majority of points representative of fresh waters was localized above the calcite–dolomite dissolution line (in Barbieri et al., 2005), conversely to thermal waters that are localized in calcite dissolution domain.

5. Discussion

5.1. Recharge and origin of salinity

In spite of an uniform low precipitation pattern of about 150 mm per year over the Lakhssas Plateau of the Anti-Atlas Mountains, the data showed remarkable water-quality variations between the northern and southern parts of the basin. While the southern water was characterized by a low salinity Ca–Mg–HCO_3 composition, water from the northern, western, and eastern margins of the basin had much higher salinity, with chloride content up to 800 mg/L (Fig. 14). This change in salinity was also associated with different stable-isotope composition, as the low-salinity groundwater from the southern area was depleted in ^{18}O and ^2H. Given the lack of spatial differentiation in precipitation, these differences could be derived from (1) different elevation; (2) modification due to recharge pathways; and (3) different timing and climate conditions of recharge (i.e., wet versus arid conditions).

The correlation of chloride with other constituents in the water such as Ca, Mg, SO_4, HCO_3 and Na (Fig. 7 and 8) in the northern

Table 1
Major-ion data for groundwater samples collected from 2008 to 2010 in the Lakhssas Plateau .

Code	Name	Nature	Date	T °C	pH	EC (μs/cm)	Ca (mg/L)	Mg (mg/L)	Na (mg/L)	K (mg/L)	HCO_3 (mg/L)	Cl (mg/L)	SO_4 (mg/L)	NO_3 (mg/L)	SiO_2 (mg/L)	TDS (mg/L)	Mg/Ca (molar)	Saturation index			
																		Cal	Dol	An	Gyp
Thermal Spring																					
M8-19	Abeino	Spring	07/10/2008	37.5	7.5	3350	571	104	185	16	250	291	1546	1		2964	0.30	0.95	1.57	−0.27	−0.12
M9-18	Lalla Mellouka	Spring	02/01/2009	35.0	7.8	2850	530	86	51	21	220	39	1576	3	17.12	2480	0.27	1.12	1.86	−0.28	−0.10
M9-19	Abeinou	Spring	03/01/2009	36.7	6.9	3470	548	88	211	27	244	265	1503	1	14.79	2830	0.27	0.36	0.35	−0.29	−0.13
M10-18	Lalla mellouka	Spring	04/05/2010	36.3	6.8	2710	604	105	52	21	220	43	1580	1		2624	0.29	0.24	0.13	−0.24	−0.07
M10-19	Abeino	Spring	04/05/2010	37.6	7.1	3430	570	97	145	25	244	277	1576	5		2937	0.28	0.55	0.76	−0.26	−0.11
South Lakhssas																					
M8-04	Timoulay Oufella	Spring	07/10/2008	25.7	7.7	845	91	40	23	3	300	43	120	14		634	0.73	0.60	1.19	−1.74	−1.52
M8-17	Timoulay izdar	Spring	07/10/2008	24.0	7.6	784	74	42	24	3	306	46	75	19		588	0.94	0.41	0.92	−2.01	−1.78
M8-22	Lahrime	Spring	07/10/2008	22.8	7.6	648	58	37	20	2	310	44	18	19		507	1.06	0.33	0.79	−2.70	−2.47
M8-21	Bouizakarne	Well	07/10/2008	22.8	7.6	837	82	43	27	2	390	55	36	18		652	0.87	0.55	1.13	−2.30	−2.70
M8-20	Tagant	Spring	07/10/2008	23.8	7.5	867	74	47	35	3	464	71	20	29		742	1.06	0.49	1.12	−2.61	−2.39
M8-23	Assaka	Spring	07/10/2008	22.5	7.2	691	62	36	24	2	305	50	21	19		519	0.96	−0.05	−0.01	−2.60	−2.37
M9-17	Timoulay izdar	Spring	02/01/2009	23.6	7.5	750	66	35	23	3	305	30	60	17	4.92	487	0.58	0.27	0.61	−2.13	−1.90
M9-20	Tagant	Spring	03/01/2009	23.3	7.6	840	70	40	34	2	354	67	49	26	5.81	569	0.89	0.42	0.92	−2.22	−1.99
M9-21	Bouizakarne	Well	03/01/2009	17.0	8.0	760	69	38	24	2	378	38	37	18	4.96	532	0.95	0.74	1.47	−2.33	−2.08
M9-23	Assaka	Spring	03/01/2009	21.5	7.6	671	59	32	24	2	305	40	22	22	5.14	459	0.91	0.32	0.67	−2.59	−2.36
M9-22	Lahrime	Spring	03/01/2009	22.6	7.6	630	57	31	21	1	317	35	21	16	5.04	439	0.92	0.33	0.73	−2.63	−2.40
M10-04	Timoulay ofella	Spring	04/05/2010	25.2	7.6	807	94	38	23	3	305	39	124	15		641	0.68	0.49	0.94	−1.71	−1.49
M10-10	Aghmad	Spring	04/05/2010	22.2	7.6	617	60	32	24	1	305	43	22	21		508	0.90	0.33	0.71	−2.58	−2.35
M10-17	Timoulay izdar	Spring	04/05/2010	23.8	7.4	869	94	36	35	4	329	67	96	32		694	0.64	0.35	0.63	−1.82	−1.60
M10-20	Tagant	Spring	04/05/2010	23.9	7.5	1000	92	44	45	3	354	107	50	42		735	0.80	0.45	0.91	−2.13	−1.90
M10-21	Bouizakarne	Well	04/05/2010	23.7	7.9	860	89	43	29	4	342	59	96	16		677	0.81	0.82	1.66	−1.86	−1.63
M10-22	Lahrime	Spring	04/05/2010	22.6	7.5	622	59	32	20	2	256	43	17	19		447	0.91	0.18	0.41	−2.70	−2.47
M10-23	Assaka	Spring	04/05/2010	22.1	7.5	791	67	41	34	3	354	71	35	21		626	1.02	0.30	0.70	−2.37	−2.14
North Lakhssas																					
M8-16	Mirkht	Spring	07/10/2008	23.0	7.5	1070	140	51	33	3	537	71	13	26		874	0.61	0.79	1.46	−2.58	−2.35
M8-15	ighrem	Spring	07/10/2008	24.3	7.1	980	100	50	33	2	500	68	18	21		791	0.83	0.25	0.54	−2.54	−2.31

M8-14	Talaint	Spring	07/10/2008	24.3	7.0	975	107	60	36	2	476	68	18	20		787	0.30	−0.05	1.00	−3.01	−2.79
M8-13	Reggada	Spring	07/10/2008	24.1	7.1	998	100	59	42	2	488	78	18	21		808	0.98	0.23	0.57	−2.57	−2.34
M9-13	Reggada	Spring	02/01/2009	23.9	7.3	1000	89	46	38	3	476	68	23	30	5.15	690	0.71	0.39	0.83	−2.48	−2.26
M9-14	Talaaint	Spring	02/01/2009	24.0	7.3	970	90	47	34	2	476	60	21	19	5.35	663	0.87	0.34	0.72	−2.51	−2.29
M9-16	Mirkht	Spring	02/01/2009	22.7	7.7	1050	114	40	30	2	537	60	18	34	5.80	703	0.86	0.90	1.67	−2.49	−2.26
M9-24	Aghbalou ouijjane	Spring	23/01/2009	25.8	7.2	1038	79	45	55	3	439	117	53	30	5.60	720	0.96	0.24	0.59	−2.17	−1.95
M10-01	Tamazzerte	Spring	03/05/2010	25.0	8.0	1006	81	49	53	3	427	99	32	25		769	1.01	0.98	2.00	−2.38	−2.16
M10-02	Anamer	Spring	03/05/2010	21.9	7.1	1110	137	34	40	4	512	92	18	41		878	0.41	0.32	0.36	−2.43	−2.20
M10-13	Reggada	Spring	03/05/2010	23.5	7.2	1440	118	66	74	3	500	186	44	46		1038	0.93	0.34	0.77	−2.15	−1.92
M10-14	Talaint	Spring	04/05/2010	24.0	7.1	1060	101	50	48	2	476	99	19	36		831	0.82	0.20	0.44	−2.53	−2.30
M10-15	Ighrem	Spring	05/05/2010	24.0	7.2	984	101	49	35	2	512	69	13	25		806	0.81	0.36	0.74	−2.69	−2.46
M10-16	Mirkht	Spring	06/05/2010	22.8	7.2	1157	162	30	45	2	512	94	18	74		938	0.31	0.57	0.73	−2.36	−2.14
M10-24	Aghbalou ouijjane	Spring	03/05/2010	29.6	7.2	1081	82	53	60	3	427	117	34	24		801	1.07	0.22	0.64	−2.33	−2.14
M10-37	Bounnaamane	Well	05/05/2010	27.2	7.0	1410	144	53	68	4	598	151	26	39		1083	0.62	0.35	0.66	−2.29	−2.08
Kerdous Spring																					
M9-25	Tanout	Spring	23/01/2009	22.9	7.2	1762	83	96	136	8	598	277	82	27	8.20	1187	**1.08**	0.29	0.98	−2.09	−1.86
M9-26	Tanout	Well	23/01/2009	21.0	7.6	1996	94	73	149	7	549	342	94	37	5.88	1232	**1.00**	0.59	1.38	−1.96	−1.73
M9-27	Association Tamacht	Well	23/01/2009	25.2	7.1	1695	86	43	189	2	390	320	73	31	15.57	1041	0.83	0.01	0.08	−2.04	−1.82
M10-09	Barrage anzi	Well	03/05/2010	23.2	7.4	1301	86	31	160	4	378	188	47	40		934	0.60	0.29	0.46	−2.19	−1.97
M10-25	Tanout	Spring	03/05/2010	22.7	7.2	2940	222	81	158	10	476	616	82	27		1672	0.61	0.52	0.93	−1.74	−1.51
Ifni Spring																					
M10-03	Esboya	Well	05/05/2010	22.3	7.0	3490	202	99	335	12	390	820	134	71		2064	0.82	0.21	0.44	−1.61	−1.38
M10-05	Sidi med youssef	Spring	05/05/2010	27.7	7.8	1631	110	50	114	5	378	295	53	30		1035	0.75	0.83	1.70	−2.08	−1.87
M10-06	Bouguerfa	Spring	05/05/2010	23.6	7.9	2020	96	35	103	16	183	202	278	92		1153	0.61	0.54	0.97	−1.44	−1.22
M10-11	Laouina	Spring	05/05/2010	22.9	7.4	3240	202	86	214	4	342	581	59	62		1550	0.71	0.55	1.05	−1.91	−1.69
M10-38	Agadir izdar	Well	05/05/2010	22.1	7.6	2280	139	57	151	5	305	474	44	33		1208	0.68	0.60	1.13	−2.11	−1.88
M10-40	Aglou	Spring	05/05/2010	23.1	7.4	3370	208	95	236	5	305	831	123	40		1843	0.76	0.51	1.01	−1.62	−1.39

Table 2
Trace-element and isotope data for groundwater samples collected from 2008 to 2010 in the Lakhssas Plateau.

Code	Name	Br (mg/L)	Br/Cl (molar)	Sr (mg/L)	$^{87}Sr/^{86}Sr$	δ^2H (‰)	$\delta^{18}O$ (‰)	d-excess (‰)	altitude (m.a.s.l)	d ^{13}C (‰PDB)	$A^{14}C$ (pcm)	$A^{14}C$ error (pcm)
Thermal Spring												
M8-19	Abeino					−37.7	−6.13	11.35	433	−5.70	6.4	0.1
M9-18	Lalla Mellouka	0.07	0.00074	13.38	0.708905				839			
M9-19	Abeinou	0.08	0.00013	14.26	0.708979				433			
M10-18	Lalla mellouka					−53.4	−7.62	7.61	839			
M10-19	Abeino					−34.1	−5.33	8.49	433			
South Lakhssas												
M8-04	Timoulay Oufella					−36.3	−5.74	9.66	811	−10.27	53.1	0.2
M8-17	Timoulay izdar					−34.3	−5.88	12.79	668	−10.68	54.6	0.2
M8-22	Lahrime					−34.1	−5.93	13.33	901	−10.73	57.5	0.2
M8-21	Bouizakarne					−33.8	−5.60	11.01	663	−10.69	58.3	0.2
M8-20	Tagant					−35.3	−5.74	10.60	541	−10.33	62.6	0.2
M8-23	Assaka					−35.3	−5.84	11.48	801	−10.40	60.6	0.2
M9-17	Timoulay izdar	0.13	0.00193	5.56	0.709394				668			
M9-20	Tagant	0.25	0.00164	3.01	0.709652				541			
M9-21	Bouizakarne	0.17	0.00195	1.99	0.709965				663			
M9-23	Assaka	0.20	0.00225	1.41	0.710257				801			
M9-22	Lahrime	0.18	0.00232	1.41	0.709946				901			
M10-04	Timoulay ofella					−33.6	−5.67	11.77	811			
M10-10	Aghmad					−34.4	−5.56	10.07	900			
M10-17	Timoulay izdar					−33.8	−5.65	11.45	668			
M10-20	Tagant					−33.7	−5.67	11.63	541			
M10-21	Bouizakarne					−33.7	−5.50	10.31	663			
M10-22	Lahrime					−34.0	−5.88	13.04	901			
M10-23	Assaka					−35.0	−5.88	12.06	801			
North Lakhssas												
M8-16	Mirkht					−31.5	−5.45	12.13	718	−7.54	40.3	0.2
M8-15	ighrem					−31.8	−5.50	12.17	682	−10.01	44.3	0.2
M8-14	Talaint					−33.5	−5.48	10.30	381	−9.84	48.5	0.2
M8-13	Reggada					−30.3	−5.42	13.03	381	−9.63	50.1	0.2
M9-13	Reggada	0.28	0.00185	1.78	0.710015				381			
M9-14	Talaaint	0.31	0.00232	1.68	0.710019				381			
M9-16	Mirkht	0.34	0.00252	2.16	0.709649				718			
M9-24	Aghbalou ouijjane	0.42	0.00158	2.10	0.710489				343			
M10-01	Tamazzerte					−30.8	−5.34	11.96	350			
M10-02	Anamer					−31.9	−5.74	13.98	643			
M10-13	Reggada					−31.5	−5.28	10.76	381			
M10-14	Talaint					−31.1	−5.22	10.70	381			
M10-15	Ighrem					−31.1	−5.09	9.69	682			
M10-16	Mirkht					−28.1	−4.86	10.77	718			
M10-24	Aghbalou ouijjane					−30.6	−5.21	11.10	343			
M10-37	Bounnaamane					−28.4	−4.89	10.79	411			
Kerdous Spring												
M9-25	Tanout	0.93	0.00150	3.62	0.710474				280			
M9-26	Tanout	1.17	0.00152	5.24	0.710065				285			
M9-27	Association Tamacht	0.71	0.00098	5.08	0.713000				500			
M10-09	Barrage anzi					−23.8	−4.23	10.03	496			
M10-25	Tanout					−28.8	−4.78	9.43	285			
Ifni Spring												
M10-03	Esboya					−21.0	−3.89	10.12	388			
M10-05	Sidi med youssef					−21.2	−3.97	10.51	450			
M10-06	Bouguerfa					−22.3	−4.68	15.16	440			
M10-11	Laouina					−28.2	−4.66	9.16	278			
M10-38	Agadir izdar					−24.0	−3.83	6.61	296			
M10-40	Aglou					−28.4	−5.10	12.40	278			

water as well as in the western and eastern margins is related to the local geology. The northern, eastern, and western sections of the Lakhssas Plateau are associated with schist rocks either overlying the Lower Cambrian carbonate rocks (northern section) or underlying in the form of the Proterozoic schist-gneiss basement (eastern and western margin, see Fig. 2 and 3). The study of Krimissa et al. (2004) suggested that the high chloride content (up to 4300 mg/L) of groundwater from the Chtouka-Massa plain, north of the Lakhssas Plateau, was derived from weathering of biotite mineral and unidentified chloride minerals in the schist rocks. This interpretation was based on actual measurements of high chloride contents of the schist rocks leachates. One of the parameters that characterized the high saline groundwater in the Chtouka-Massa plain was the relatively low Na/Cl ratio (Krimissa et al., 2004). This geochemical observation is consistent with our data that showed relatively low Na/Cl (i.e., lower than unity or seawater ratio) in the saline water from the Lakhssas Plateau (Fig. 8). In addition, the northern water had significantly higher silica concentrations

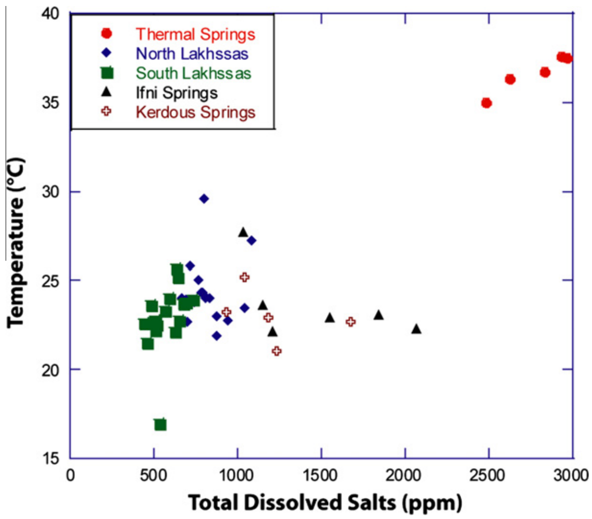

Fig. 5. Relationship between temperature and total dissolved salts. Samples are sorted according to their geographical distribution.

(Fig. 15) that could reflect interactions with igneous rocks. Furthermore, the northern waters with the highest chloride (and silica) contents had also lower Br/Cl ratios ($<1.5 \times 10^{-3}$), which was consistent with the relatively lower Br/Cl ratios in schist-salinized water reported by Krimissa et al. (2004). Thus, the combination of high silica and low Na/Cl and Br/Cl ratios of the saline water suggests that mineralization of the associated schist rocks played a role in salinization of water resources along the northern, western and eastern margins of the Lakhssas Plateau.

In contrast, the low salinity of the southern water was associated with predominantly carbonate rocks without possible salinity effects of the schist rocks. It is also possible that the schist cover in the northern margin reduces the permeability of the unsaturated zone, leading to higher evaporation during recharge while unsaturated zone composed of only carbonate rocks in the south has much higher permeability and less evaporation and potential isotopic fractionation.

In addition to salinity, the northern and Ifni (western margin) waters had higher δ^2H and δ^{18}O values relative to the southern water and thermal water; although all groups had δ^2H–δ^{18}O slopes and deuterium excess values close to the GMWL and the Local Meteoric Water Line (Fig. 9). The meteoric slope ($\sim$8) rules out evaporation as a major salinisation process. The differences in the δ^2H and δ^{18}O values between the different waters in the Lakhssas basin could be related to the elevation of the recharge area. Fig. 16 shows the relationships between sample elevation and δ^{18}O values, as compared to the isotopic regional gradient established by Cappy (2006) in the Upper Drâa catchment in the southern part of the High Atlas Mountains. This study showed clear relationships between elevation and stable isotope composition of precipitation along a 320 km transect close to the study area. Thus, the relative heavy-isotope depletion of the southern water is related to the higher elevation (Fig. 16) of the recharge water relative to recharge into the northern part of the basin.

Finally, the thermal water, which is also located in the southern part of the basin, had significantly different chemical and isotopic compositions. The predominance of Ca and SO_4 (Ca/SO_4 ratio $\sim$0.8), moderate levels of HCO_3 and the high Sr/Ca suggest that the dissolved constituents of the thermal waters were derived from calcium–sulfate (gypsum, anhydrite) and calcium carbonate dissolution. Evidence for Lower Cambrian evaporites was reported in Benssaou and Hamoumi (2004). Alternatively, one could suggest that the high sulfate concentration in the thermal water were derived from oxidation of sulfides in a process in which H_2S and CO_2 degased from the subsurface and were converted into sulfate and bicarbonate (e.g. White et al., 1971). Yet given that the Ca/SO_4 ratio was close to unity, that Ca and SO_4 represented 77% of the dissolved constituents, and the high Sr/Ca ratio that characterizes

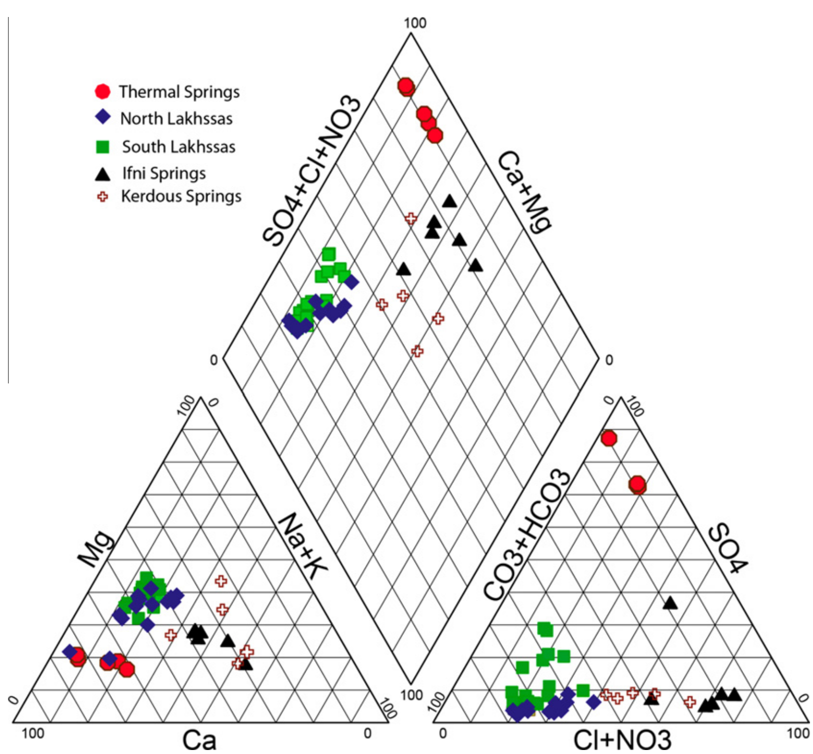

Fig. 6. Piper trilinear diagram. Samples are sorted according to their geographical distribution.

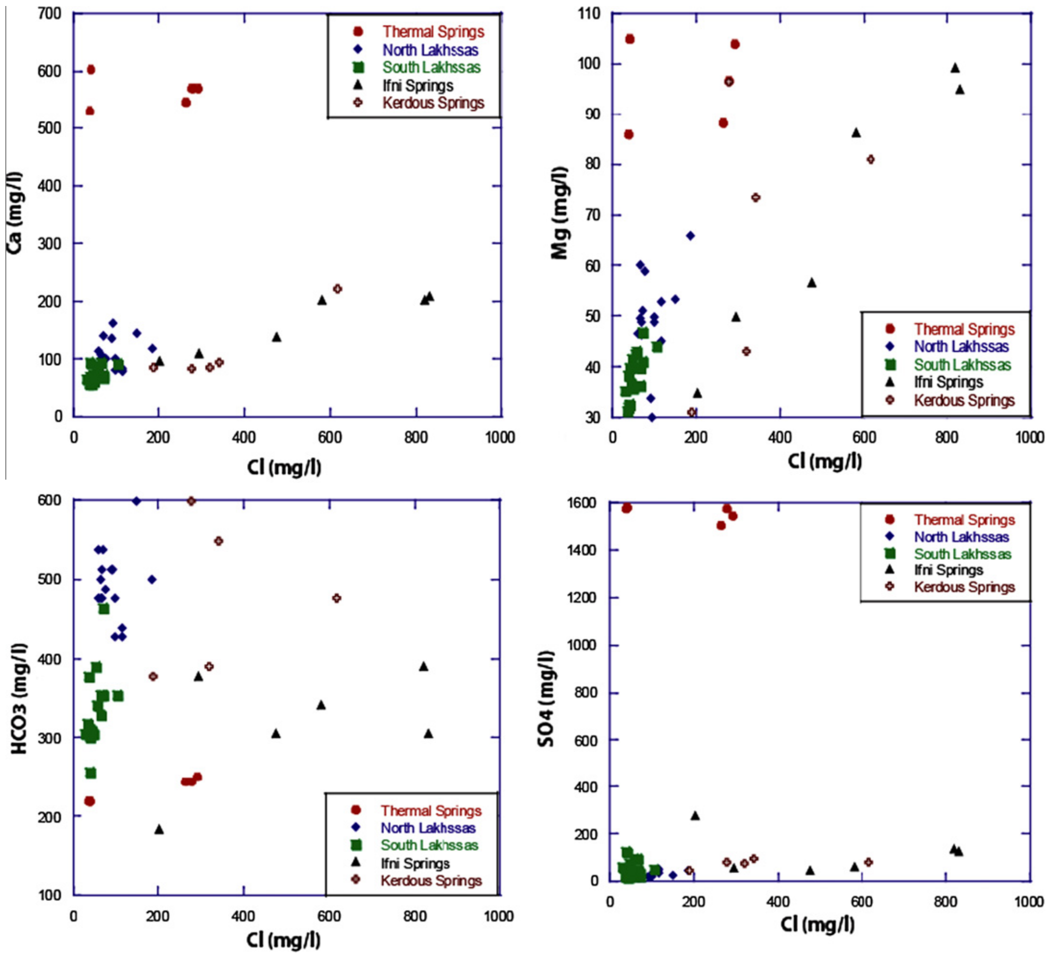

Fig. 7. Calcium, magnesium, bicarbonate and sulfate concentrations (mg/L) versus chloride concentration (mg/L) of groundwater. Samples are sorted according to their geographical distribution.

gypsum mineral, we privilege the hypothesis of sulfate mineral dissolution. The thermal water was also characterized by much more ^{2}H and ^{18}O depleted isotopic composition (Fig. 9) that indicates a different water origin, presumably from past recharge under colder and more humid conditions than present ones.

5.2. Water–rock interactions

This study utilizes strontium isotope geochemistry as a tool to evaluate the role of water–rock interactions on the water solutes. Our analysis was based on the assumption that the different rock formations in Lakhssas Plateau (Fig. 2 and 3) had distinctive $^{87}Sr/^{86}Sr$ ratios: (1) the underlying Proterozoic crystalline (granitoide and metamorphic) basement with expected radiogenic high $^{87}Sr/^{86}Sr$ (>0.711); (2) the Lower Cambrian limestone and/or anhydrite with expected $^{87}Sr/^{86}Sr$ ratio of ~0.7089 that represents the seawater secular Sr isotope ratio for the Early Cambrian Period (Montañez et al., 2000); (3) the overlying Middle–Upper Cambrian schist rocks with expected radiogenic high $^{87}Sr/^{86}Sr$ (>0.710). The Sr isotope data of the groundwater from the Lakhssas Plateau indicated that only the thermal water had a $^{87}Sr/^{86}Sr$ ratio that was consistent with the expected $^{87}Sr/^{86}Sr$ ratio of Early Cambrian seawater as manifested itself either in carbonates or evaporates. In contrast, both the northern and southern water types showed higher $^{87}Sr/^{86}Sr$ ratios (0.7094 to 0.71048; Fig. 12), inferring contribution of *both* Early Cambrian carbonates and schist rocks with higher $^{87}Sr/^{86}Sr$ ratios. One sample (M9-27) collected near the eastern margin of the basin close to Kerdous Inlier had very high $^{87}Sr/^{86}Sr$ ratio of 0.7130, which indicated predominant contribution of solutes originated from interactions with the schist rocks.

The variations of $^{87}Sr/^{86}Sr$ ratios with respect to Mg/Ca ratios (Fig. 17) suggest that the chemistry of groundwater from both the northern and southern areas was controlled by mixing relationships between two end-members with low and high $^{87}Sr/^{86}Sr$–Mg/Ca ratios. We assumed that the low $^{87}Sr/^{86}Sr$ and Mg/Ca end-member, as represented by the thermal water, was derived from dissolution of Early Cambrian limestone, while the high $^{87}Sr/^{86}Sr$ and Mg/Ca end-member was derived from mineralization of schist rocks. The average Mg/Ca molar ratios measured in saline groundwater from the Chtouka-Massa plain that apparently was salinized by mineralization of schist rocks (Krimissa et al., 2004, Krimissa, 2005) was 1.9, which corresponds to the Schist end-member (marked as "S" in Fig. 17). Alternatively, one may argue that the dolomite component in the aquifer also had a relatively higher $^{87}Sr/^{86}Sr$ ratio (marked as "D" in Fig. 17), and thus the trend observed in the groundwater reflects the mixing relation between solutes originated from limestone (low Mg/Ca and $^{87}Sr/^{86}Sr$) and dolomite (high Mg/Ca and $^{87}Sr/^{86}Sr$) dissolution. If that was the case, the $^{87}Sr/^{86}Sr$ modification in the dolomite rocks relative to the original composition of the marine limestone could be generated by secondary dolomitization with solutions having higher $^{87}Sr/^{86}Sr$ ratios relative to the composition of the Early Cambrian limestone.

Finally, the balance between the sum of calcium and magnesium as compared to DIC, which was composed primarily of HCO_3^-, showed an excess of Ca^{2+} and Mg^{2+} relative to HCO_3^- (Fig

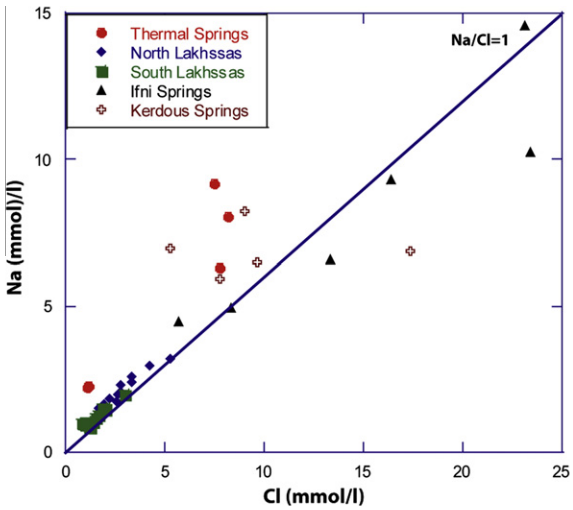

Fig. 8. Relationship between sodium concentration (mol/L) and chloride concentration (mol/L) of groundwater. Samples are sorted according to their geographical distribution.

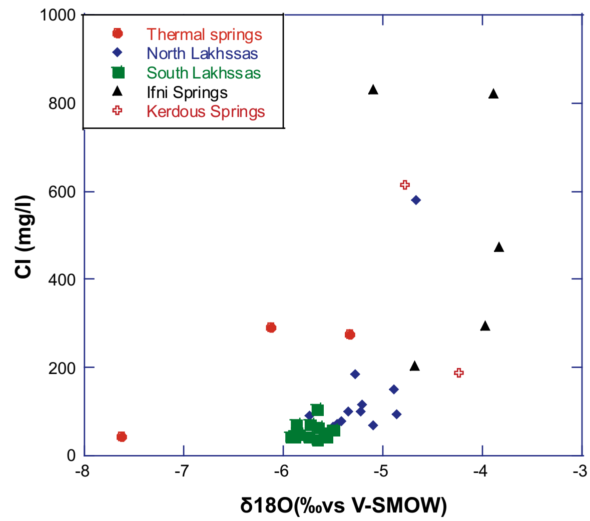

Fig. 10. Relationship between chloride concentration and $\delta^{18}O$. Samples are sorted according to their geographical distribution.

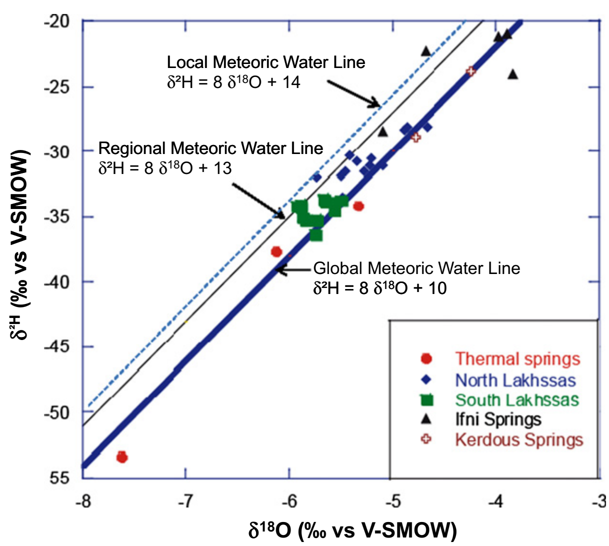

Fig. 9. Relationship between δ^2H and $\delta^{18}O$. Samples are sorted according to their geographical distribution. The Global Meteoric Water Line, Moroccan Meteoric Water Line and Local Meteoric Water Line are reported.

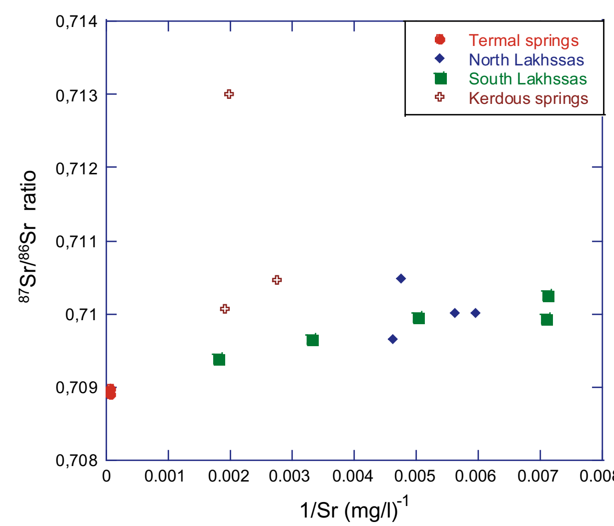

Fig. 11. Strontium isotope ratios ($^{87}Sr/^{86}Sr$) versus 1/Sr concentrations $(mg/L)^{-1}$. Samples are sorted according to their geographical distribution.

18). At the same time the Ca/HCO_3^- ratios were typically lower than unity, inferring that dissolution of limestone alone could not account for the calcium and magnesium excess. One possible explanation was that the calcium and magnesium excess was derived from mineralization of the non-carbonate fraction such as the schist rocks. This was particularly shown in the northern and Ifni (eastern margin) waters that are associated with schist rocks relative to the southern water that seemed to be in equilibrium with mostly carbonate rocks.

5.3. Residence time

Carbon-isotope measurements ($A^{14}C$ and $\delta^{13}C$) of dissolved inorganic carbon (DIC, mainly HCO_3^-) were used to provide information on the apparent residence time of groundwater in the Lakhssas Plateau. The relationships between $A^{14}C$ and $\delta^{13}C$ are illustrated in Fig. 11. The data showed lower $A^{14}C$ and higher $\delta^{13}C$ values ($n = 4$) in the northern groundwater ($A^{14}C$ of 40–50 pmC, $\delta^{13}C$ of −7.5–10‰ V-PDB) and higher $A^{14}C$ (54 to 63 pmC) and lower $\delta^{13}C$ values (−10.5 ± 1‰ V-PDB) in the southern groundwater. In contrast, the thermal water showed much lower $A^{14}C$ (6 pmC) and higher $\delta^{13}C$ (−5.7‰ V-PDB). In addition, the northern waters had higher DIC contents relative to the southern waters (Fig. 18).

In the semi-arid ecosystem of the Anti-Atlas, the vegetation is rather sparse, mainly consisting of some argan trees. The $\delta^{13}C$ values of such plants (Calvin, C3, photosynthesis cycle) would be close to −27‰ V-PDB (Clark and Fritz, 1997). Bacterial decay of organic matter in the soil produces CO_2 that has initially the same $\delta^{13}C$ values. However, the partial diffusion of soil CO_2 towards the atmosphere leads to enrichment by about 4‰ of the fraction that remains in the soil ($\delta^{13}C \sim -23$‰ V-PDB). Finally, during the hydration of soil CO_2 to aquatic $CO_2(aq)$ and dissociation of $CO_2(aq)$ to HCO_3^-, the carbon isotopes fractionate again, resulting in ^{13}C enrichment in the dissolved bicarbonate (Douglas et al., 2006; Fontes, 1992; Gonfiantini and Zuppi, 2003; Mook, 1980; Mahlknecht et al., 2006; Salomon and Mook, 1986), which depends on pH and temperature. At 25 °C and neutral pH, the net isotopic fraction-

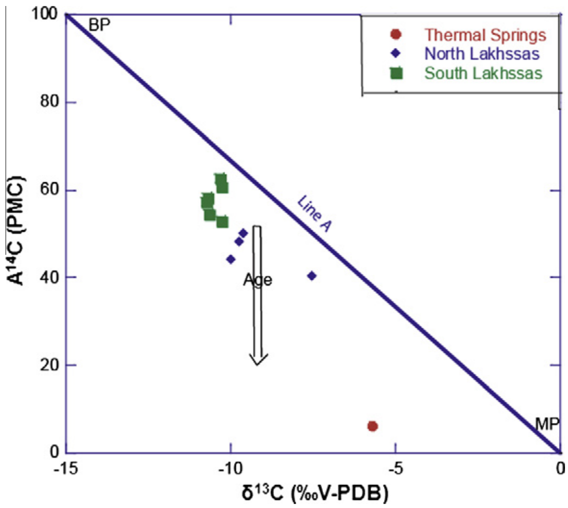

Fig. 12. Relationship between $\delta^{13}C$ and $A^{14}C$ for some north and south springs of the Lakhssas Plateau. The line represents a theoretical closed-system mixing between modern DIC (PB: $A^{14}C$ = 100 pmC and $d^{13}C$ = −15‰ V-PDB) and marine carbonate rock (PM: $A^{14}C$ = 0 pmC and $d^{13}C$ = 0‰ V-PDB). The arrow indicates the effect of an increase of residence time.

ation is estimated as ~8‰ (Appelo and Postma, 1993; Clark and Fritz, 1997), and thus C3 plants are expected to generate HCO_3^- with $\delta^{13}C \sim -15$‰ V-PDB.

Consequently, we modeled the DIC isotopic variations as mixing between (1) DIC originated from soil CO_2 and conversion to HCO_3^- with modern $A^{14}C$ = 100 pmC and $\delta^{13}C \sim -15$‰; and (2) DIC originated from dissolution of the Early Cambrian limestone and/or dolomite with $A^{14}C \sim 0$ pmC and $\delta^{13}C \sim 0$‰. Line A in Fig. 12 represents the possible mixing relationship between these two end-members. In order to calculate the apparent residence time of the groundwater, we used the decay equation of ^{14}C corrected for the mixing model. This approach is known as the IAEA model (Salem et al., 1980). In addition, we used two other isotope-exchange models; the Fontes and Garnier's model (Fontes and Garnier, 1979), which takes into account the exchange of DIC with either the biogenic CO_2 or the solid carbonate phase, and the Eichinger's model (Eichinger, 1983), which can be useful in the case of strong exchange with the solid phase. The three models being more or less sensitive to the different estimated parameters, their joint use allows giving an idea of the uncertainties on groundwater "ages". For all these models we assumed a closed system condition, and the ^{13}C fractionation factors were calculated using the measured values of pH and temperature for each sample.

The age-dating results of the three models are presented in Table 3. The computed mean residence times (MRT) of the low-temperature groundwater from the Lakhssas Plateau depend on the used model. They are close to 0 (mathematically negative) for the Fontes and Garnier's model and range from 800 to 3400 yrs BP for the IAEA model, with very small differences between the southern groundwater (800–2200 yrs BP) and the northern groundwater (1900–3400 yrs BP). These differences are more pronounced for the Eichinger's model; the southern groundwater would be recently recharged (0–200 yrs BP), while the MRT of northern groundwater range from 800 to 2000 yrs BP. These divergences between the models are very often observed when the effects of radioactive decay on the ^{14}C concentration of DIC are limited compared to those of water–rock interaction that induce changes in ^{14}C balance, which seems to be the case for the low-temperature groundwater from the Lakhssas Plateau. However, the results suggest some contribution of relatively old groundwater (a few thousands of years) to the sampled springs and wells, particularly in the northern part of the basin.

The thermal water in the southern part of the Lakhssas Plateau, originating from a much more depleted ^2H and ^{18}O recharge, had a significant higher radiocarbon age of 10–15 ka BP, depending on the used model. This is consistent with what is known about the return to wetter conditions in Northern Africa during the last deglaciation period (e.g. Gasse, 2000, and references therein) and infers a much older recharge of the geothermal water.

6. Conclusions

This study provides a detailed evaluation of the hydrochemistry and isotope geochemistry (O, H, C, Sr) of groundwater from the carbonate Lakhssas Plateau in the Anti-Atlas Mountains of southwestern Morocco. Integration of the geochemical data indicated that the water quality and hydrochemistry of the groundwater originated primarily from water–rock interactions with the aquifer rocks. The integrated data indicated two types of groundwater (1) low-temperature groundwater that originated from the Atlantic Ocean moisture with similar stable-isotope composition to modern rain; and (2) thermal water in the southern part of the basin that originated from a much more heavy-isotope depleted precipitation.

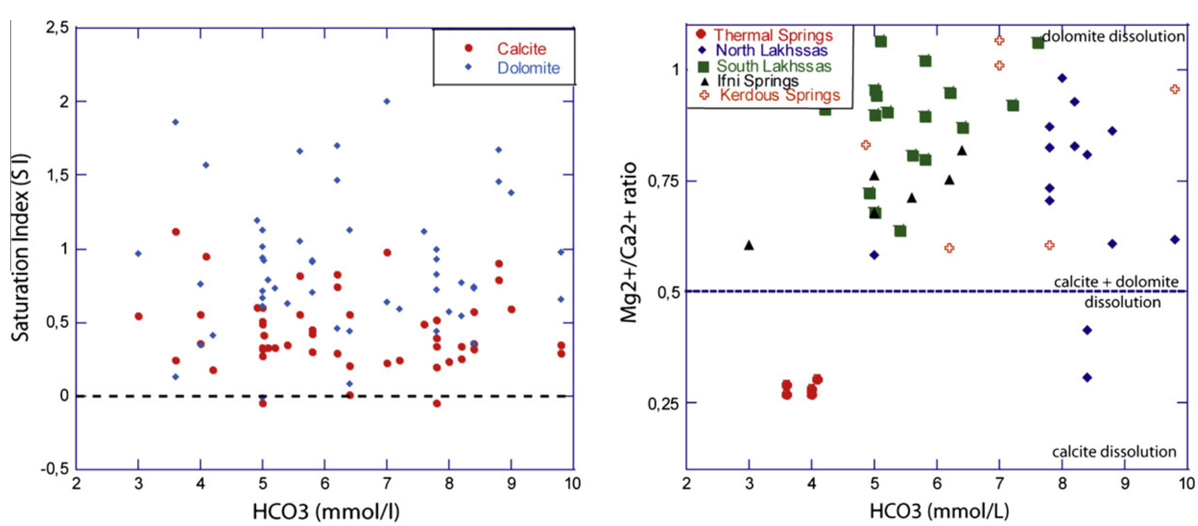

Fig. 13. Saturation index of calcite and of dolomite versus HCO_3^- and Mg^{2+}/Ca^{2+} molar ratio versus HCO_3^-.

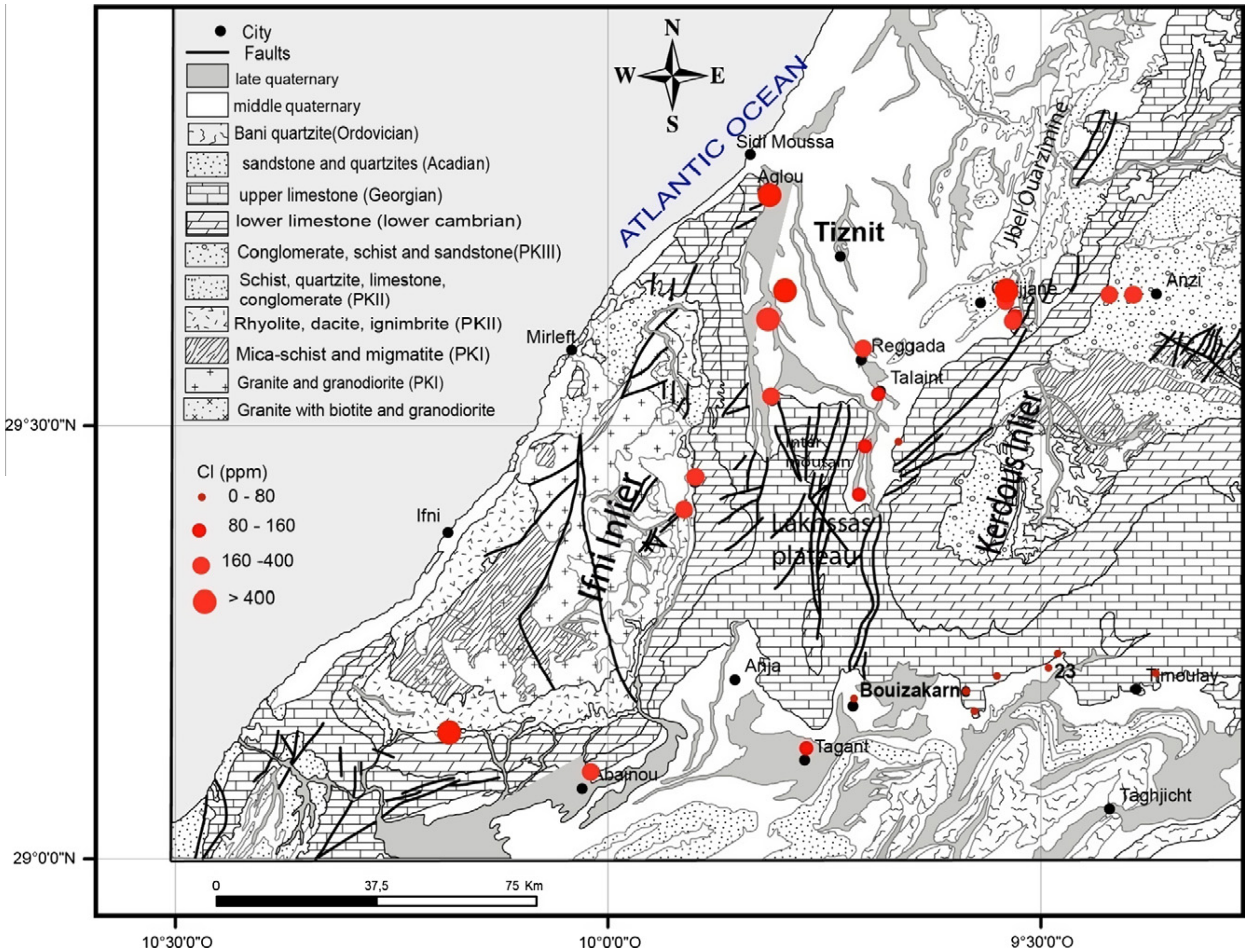

Fig. 14. Salinity map of the Lakhssas Plateau groundwater showing water quality difference between the northern and southern parts of the basin.

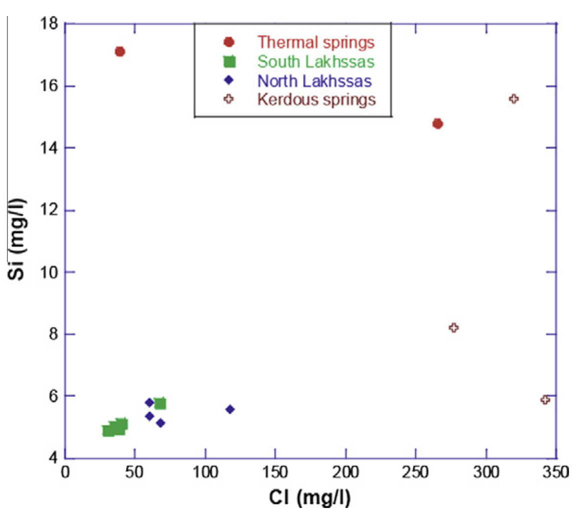

Fig. 15. Variation of silica (mg/L) versus chloride (mg/L) concentrations of groundwater. Samples are sorted according to their geographical distribution.

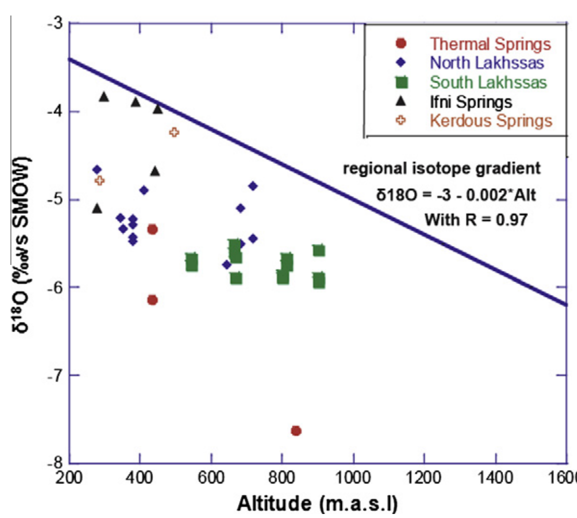

Fig. 16. Relationship between $\delta^{18}O$ in groundwater and the elevation of the sampled springs and wells.

For the low-temperature groundwater, the higher elevation towards the south induced stable isotope fractionation effects that resulted in relatively low δ^2H and $\delta^{18}O$ values. The salinity of groundwater from the western, northern, and eastern margins of the basin was higher than that of the southern waters. The Sr isotope data coupled with variations of major element ratios such as Na/Cl, Br/Cl, and Mg/Ca suggest that the high salinity was related to mineralization of schist rocks that are abundant at western, northern, and eastern margins of the basin but not at

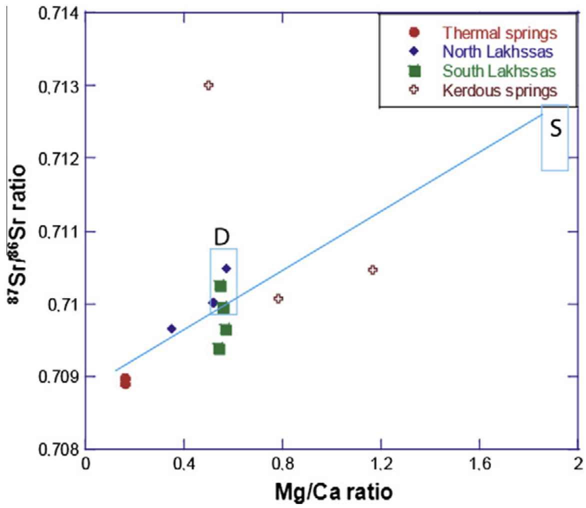

Fig. 17. Variation of $^{87}Sr/^{86}Sr$ ratio versus Mg/Ca ratio of groundwater. Samples are sorted according to their geographical distribution.

the southern part, where the aquifer is composed of only carbonate rocks. The majority of the water chemistry and Sr isotopes were controlled by equilibrium with limestone and dolomite rocks, whereas interactions with schist rocks increased the content of the dissolved constituents (including dissolved silica) with a strong radiogenic $^{87}Sr/^{86}Sr$ fingerprint. The water in the south had lower $\delta^{13}C$ and higher $A^{14}C$ values relative to the northern water, which could be due to water–rock interactions. However, among the three ^{14}C age models that were used, the Eichinger's model computed longer mean residence time for the northern groundwater (1–2 ka) than for the southern groundwater (recent). The IAEA model indicated a mean residence time of a few thousands of years for both northern and southern groundwater.

In contrast, the thermal water found in the southern part of the basin was recharged by much more ^{18}O and ^{2}H depleted water, about 10–15 ka BP, presumably under a wetter and cooler climate than at present. The thermal water interacted with Ca–sulfate (gypsum, anhydrite) and limestone rocks, leading to a $^{87}Sr/^{86}Sr$ ratio that matched the expected Sr isotope composition of the Early Cambrian seawater.

As with many other exploited basins in developing countries, information on the hydrology and sustainability of the groundwater resources in the Lakhssas Plateau in the Anti-Atlas Mountain of southwestern Morocco is limited, if exist at all. The integrated data presented in this study suggest that the groundwater in the basin did not originate only from modern recharge. In addition, the data showed large water quality differentiation with high quality water in the southern part of the basin relative to highly saline water in the northern, western, and eastern parts. Given the weakness of

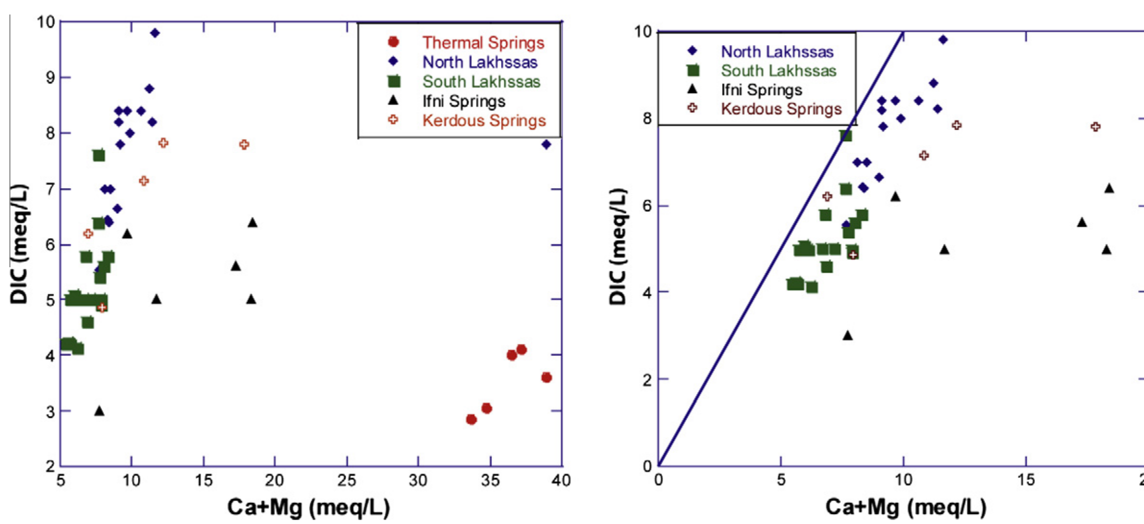

Fig. 18. Variation of DIC (meq/L) versus Ca + Mg concentration (meq/L) of groundwater. Samples are sorted according to their geographical distribution.

Table 3
Carbon isotope data, and mean residence times ("ages") calculated by three dating models: Fontes and Garnier's model (Fontes and Garnier, 1979), IAEA model (Salem et al., 1980) and Eichinger's model (1983).

Sample	Name	$A^{14}C$ DIC pmC	$\delta^{13}C$ DIC ‰ V-PDB	«Age» Fontes Garnier a BP	«Age» IAEA a BP	«Age» Eichinger a BP
Thermal water						
M9-19	Abeino	6.4	−5.7	10 000	14 000	15 300
Southern water						
M9-17	Timoulay Izdar	54.6	−10.7	<0	2200	200
M8-04	Timoulay Oufela	53.1	−10.3	<0	1700	0
M9-22	Lahrim	57.5	−10.7	<0	1900	<0
M9-21	Boui-Izakarn	58.3	−10.7	<0	1800	<0
M9-23	Assaka	60.8	−10.3	<0	1200	<0
M8-20	Tagant	62.6	−10.3	<0	800	<0
Northern water						
M9-14	Talaint	48.5	−9.8	<0	2500	1300
M9-13	Reggada	50.1	−9.6	<0	2100	800
M8-15	Ighrem	44.3	−10.0	<0	3400	2000
M8-16	Ifri	40.3	−7.5	<0	1900	1000

recent replenishment, we predict that continued exploitation of the groundwater in this semi-arid zone could further increase the salinization of the water resources, particularly in areas in the basins with presence of schist rocks.

Acknowledgements

This study is supported within the NATO Project (ESP.MD.SFPP 983134) and CNRST-CNRS collaborative Project (No. SDU/10/08). We thank the Hydraulic Agency of Souss-Mass-Draa basin for their help throughout the project. In fine, we thank the two reviewers and Editor for their constructive remarks.

References

Agence du Bassin Hydraulique du Souss-Massa-Draa, 2004. Contribution des ressources en eau au développement socio-économique dans les bassins du sud [Contribution of water resources in socio-economic development in the southern basins], 62 p.

Agence du Bassin Hydraulique du Souss-Massa-Draa, 2006. Etude d'aménagement intégré des ressources en eau du bassin de Guélmime [Study of integrated water resources management in Guélmime basin], Rapport, 40p.

Agoussine, M., 1991. Contribution a l'étude hydrogéologique de la plaine de Guelmim (Anti-Atlas occidental Marocain) Modélisation et gestion des ressources en eau. Doctorat, Univ. Cadi Ayyad, Marrakech, Maroc.

Ait Lemkademe, A., Michelot, J.L., Benkaddour, A., Hanich, A., Maliki, A., 2011. Isotopic and hydrochemical approach to the functioning of an aquifer system in the region of Marrakech (Morocco). Rapid Commun. Mass Spectrom. 25, 2785–2792.

Appelo, C.A.J., Postma, D., 1993. Geochemistry, Groundwater, and Pollution. A.A. Balkema, Rotterdam.

Azzaz, H., Cherchali, M., Meddi, M., Houha, B., Puig, J.M., Achachi, A., 2007. The use of environmental isotopic and hydrochemical tracers to characterize the functioning of karst systems in the Tlemcen Mountains, northwest Algeria. Hydrol. J. 16, 531–546.

Barbey, P., Oberli, F., Burg, J.P., Nachit, H., Pons, J., Meier, M., 2004. The Palaeoproterozoic in western Anti-Atlas (Morocco): a clarification. J. Afr. Earth Sci. 39, 239–245.

Barbieri, M., Boschetti, T., Petitta, M., Tallini, M., 2005. Stable isotope (^{2}H, ^{18}O and ^{87}Sr/^{86}Sr) and hydrochemistry monitoring for groundwater hydrodynamics analysis in a karst aquifer (Gran Sasso, central Italy). Appl. Geochem. 20, 2063–2081.

Belfoul, M.A., 2005. Cinématique de la déformation hercynienne et géodynamique de la marge NW du gondwana (Anti-Atlas Sud-Occidental, Sahara Marocain: Zemmour, Ouled Dhlim et Mauritanides septentrionales). [Kinematics of the Hercynian deformation and geodynamics of the NW Gondwana margin (South Western Anti-Atlas, Moroccan Sahara, Zemmour, Ouled Dhlim and northern Mauritanides)]. Thèse-es-sciences, Ibn Zohr University, Agadir, Morocco.

Benssaou, M., Hamoumi, N., 2004. Les microbialites de l'Anti-Atlas occidental (Maroc): marqueurs stratigraphiques et témoins des changements environnementaux au Cambrien inférieur. [The microbialites of western Anti-Atlas (Morocco): stratigraphic markers and indicators of environmental change in the Lower Cambrian]. C.R. Geosci. 336, 109–116.

British geological Survey (BGS), 2001. Carte géologique du Maroc au 1/50 000. Feuille de Had-n-Tahala. [geological map of Morocco 1/50 000. Had-n-Tahala Sheet]: Notes et Mém. Serv. Géol. No. 403, Maroc.

Bouchaou, L., Tagma, T., Michelot, J.L., Boutaleb, S., Massault, M., Hsissou, Y., Bouragba, L., ElFaskaoui, M., in press Isotopic Tracers to Study Relationship between Surface Water and Groundwater: Case of Souss Upstream Catchment (Morocco). TECDOC, IAEA, Vienna, Austria.

Bouchaou, L., Michelot, J.L., Vengosh, A., Hsissou, Y., Qurtobi, M., Gaye, C.B., Bullen, T.D., Zuppi, G.M., 2008. Application of multiple isotopic and geochemical tracers for investigation of recharge, salinization, and residence time of water in the Souss–Massa aquifer, Southwest of Morocco. J. Hydrol. 352, 267–287.

Bouchaou, L., Michelot, J.L., Qurtobi, M., Zine, N., Gaye, C.B., Aggarwal, P.K., Marah, H., Zerouali, A., Taleb, H., Vengosh, A., 2009. Origin and residence time of groundwater in the Tadla basin (Morocco) using multiple isotopic and geochemical tools. J. Hydrol. 379, 323–338.

Cappy, S., 2006. Hydrological Characterization of the Upper Drâa Catchment: Morocco. PhD Thesis, Faculty of Mathematics and Sciences, University of Bonn.

Charlot, R., 1978. Caractérisation des événements éburnéens et panafricains dans l'Anti-Atlas marocain. Apport de la méthode Rb/Sr. [Eburnean and panafricans events Characterization of Moroccan Anti-Atlas. Contribution of Rb/Sr]. PhD Thesis, Rennes University (France), 220p.

Clark, I.D., Fritz, P., 1997. Environmental Isotopes in Hydrogeology. Lewis, New York.

Craig, H., 1961. Isotopic variations in meteoric waters. Science 133, 1702–1703.

Douglas, A., Osiensky, J.L., Kent Keller, C., 2006. Carbon-14 dating of groundwater in the Palouse Basin of the Columbia river basalts. J. Hydrol. 334, 502–512.

Eichinger, L., 1983. A contribution to the interpretation of 14C groundwater ages considering the example of a partially confined sandstone aquifer. Radiocarbon 25, 347–356.

Fontes, J.Ch., 1992. Chemical and isotopic constraints on 14C dating of groundwater. In: Long, Taylor, Kra (Eds.), Radiocarbon after Four Decades. Springer-Verlag, New York.

Fontes, J.Ch., Garnier, J.M., 1979. Determination of initial ^{14}C activity of the total dissolved carbon: a review of the existing models and a new approach. Water Resour. Res. 12, 399–413.

Gasse, F., 2000. Hydrological changes in the African tropics since the Last Glacial Maximum. Quat. Sci. Rev. 19, 189–211.

Gonfiantini, R., Zuppi, G.M., 2003. Carbon isotope exchange rate of DIC in karst groundwater. Chem. Geol. 197, 319–336.

Han, G., Liu, C., 2004. Water geochemistry controlled by carbonate dissolution: a study of the river waters draining karst-dominated terrain, Guizhou Province, China. Chem. Geol. 204, 1–21.

Hassenforder, B., 1987. La tectonique panafricaine et varisque de l'Anti-Atlas dans le massif de Kerdous (Maroc). [Panafrican and Variscan Tectonics of the Anti-Atlas in the Kerdous inlier]. PhD thesis, L. Pasteur University, Strasbourg, 249p.

Krimissa, S., Michelot, J.L., Bouchaou, L., Mudry, J., Hsissou, Y., 2004. About the origin of chloride in groundwater from a coastal aquifer under semi-arid climate (Chtouka-Massa, Morocco). C.R. Géosci., Paris 336 (15), 1363–1369.

Krimissa, S., 2005. Nappes superficielles en zone semi-aride: origine des eaux et de la salinité, renouvellement: exemple des nappes massa et souss (Maroc). [Superficial aquifers in semi arid area: origin of water and salinity, renewal: the example of Massa and Souss Aquifer (Morocco)]. University Thesis, franche-comité university.

Mahlknecht, J., Garfias-Sodis, J., Tech, R.A., 2006. Geochemical and isotopic investigations on groundwater residence time and flow in the Independence Basin, Mexico. J. Hydrol. 324, 283–300.

Marfia, A.M., Krishnamurthy, R.V., Atekwana, E.A., Panton, W.F., 2004. Isotopic and geochemical evolution of ground and surface waters in karst dominated geological setting: a case study from Belize, Central America. Appl. Geochem. 19, 937–946.

Montañez, I.P., Osleger, D.A., Banner, J.L., Mac, L.E., 2000. Evolution of the Sr and C Isotope Composition of Cambrian Oceans. GSA Today, v. 10, no. 5, (May 2000).

Mook, W.G., 1980. Carbon-14 in hydrogeological studies. In: Fritz, P., Fontes, J.C. (Eds.), Handbook of Environmental Isotopes Geochemistry, vol. 1. Elsevier, Amsterdam, pp. 50–74.

Oliva, P., 1977. Karst et structures dans le plateau des Akhssas, L'Anti Atlas occidental-Maroc. [Karst and structure in the Lakhssas plateau, western Anti – Atlas, Morocco]. Réunion de karstologie, Grenoble, Revue geogr. Alpin XVI 2 et 3.

Ouda, B., El Hamdaoui, A., Ibn Majah, M., 2004. Isotopic composition of precipitation at three Moroccan stations influenced by oceanic and Mediterranean air masses. TECDOC 1453, 125–140, IAEA, Vienna, Austria.

Pique, A., Bouabdelli, M., Soulaimani, A., Youbi, N., Illiani, M., 1999. Les conglomérat du PIII (Protérozoique terminal) de l'Anti-Atlas (Sud du Maroc): molasses tardi-panafricaines, ou marqueurs d'un rifting finiprotérozoique. [The PIII conglomerate (terminal Proterozoic) of the Anti-Atlas (south Morocco): late-panafrican molasses, or markers of terminal Proterozoic rifting]. C.R. Acad. Sci., Paris 328, 409–414.

Salem, O., Visser, J.H., Dray, M., Gonfiantini, R., 1980. Environmental isotopes used in a hydrogeological study of north-eastern Brazil. In: Arid-zone Hydrology: Investigations with Isotope Techniques, IAEA, Vienna.

Salomon, W., Mook, W.G., 1986. Isotope geochemistry of carbonates in the weathering zone. In: Fritz, P., Fontes, J.C. (Eds.), Handbook of Environmental Isotopes Geochemistry, vol. 1. Elsevier, Amsterdam, pp. 239–265.

Smiler, R., 2005. Diagram, Laboratory of Hydrogeology. Avignon University, France.

Soulaimani, A., 1998. Interaction socle/couverture dans l'Anti-Atlas occidental (Maroc): rifting fini-protérozoïque et orogenèse hercynienne. [Interaction basement/cover in the western Anti-Atlas (Morocco): terminal Proterozoic rifting and Hercynian orogenesis]. thèse de doctorat d'état es-sciences 215p, Univ Cadi Ayyad, Marrakech, Maroc.

Soulaimani, A., Bouabdelli, M., Pique, A., 2003. L'extention continentale au Néo-protérozoïque supérieur cambrien inférieur dans l'Anti-Atlas (Maroc). [The continental extension at upper Neoproterozoic Lower Cambrian in the Anti-Atlas (Morocco)] Bull. Soc. Géol. France, t. 174, No. 1, pp. 83–92.

Soulaimani, A., Bouabdelli, M., 2005. Le Plateau de Lakhssas (Anti-Atlas occidental, Maroc): Un graben fini-précambrien réactivé à l'hercynien. [Lakhssas Plateau (Western Anti-Atlas, Morocco) terminal precambrian graben reactived at the Hercynian]: Annales de la Société Géologique du Nord (Lille), v. T. 11(2ème série), pp. 177–148.

Soulaimani, A., Burkhard, M., 2008. The Anti-Atlas chain (Morocco): the southern margin of the Variscan belt along the edge of the West African craton: From: Ennih, N., Lié Geois, J.P. (Eds.), The Boundaries of the West African Craton. Geological Society, London, Special Publications, v. 297, pp. 433–452.

Raibi, F., Benkaddour, A., Hanich, L., Chehbouni, A., 2006. Caractérisation hydrogéochimique et isotopique des eaux de surface et des eaux souterraines du bassin versant de Tensift. Gestion Intégrée des Ressources en Eaux et Défis du Développement Durable (GIRE3D), Faculté des Sciences Semlalia, Marrakech, Morocco.

White, D.E., Muffler, L.P.J., Truesdell, A.H., 1971. Vapor-dominated hydrothermal systems compared with hot-water systems. Econ. Geol. 66, 75–97.